Role of impurities in the Lehmann effect of cholesteric liquid crystals: Towards an alternative model

Patrick Oswald* and Guilhem Poy
Univ Lyon, ENS de Lyon, Univ Claude Bernard, CNRS, Laboratoire de Physique, F-69342 Lyon, France

(Received 13 July 2018; published 19 September 2018)

The Lehmann effect is the rotation of cholesteric droplets when they are submitted to a temperature gradient. So far, this effect was only observed in the coexistence region between the cholesteric phase and its isotropic liquid. This zone of coexistence is due to the presence in the LC of impurities. In this paper, we show that the rotation velocity of the droplets does not depend on the choice of the impurity and on its concentration, providing that the variations of the equilibrium twist and the rotational viscosity are taken into account. These results were obtained by doping the cholesteric LC (a diluted mixture of 7CB and R811) with nonmesogenic and mesogenic impurities. The nonmesogenic impurities used are the biphenyl, the hexachloroethane, and a fluorinated polyether polymer. The mesogenic impurity is the LC I52. From these experiments we conclude that the Lehmann effect is certainly not due to a chemical torque of the type described by Leslie, Akopyan, and Zel'dovich. Finally, we propose alternative avenues that might be explored to understand the Lehmann effect.

DOI: 10.1103/PhysRevE.98.032704

I. INTRODUCTION

By doping a nematic phase with a small amount of a chiral molecule, one obtains a cholesteric phase in which the director $\vec{n}$ rotates along a space direction called the helical axis [1]. The cholesteric to isotropic phase transition is first order so that there exists a coexistence region in which the two phases coexist. In a pure LC such as 7CB (4-heptyl-4′-cyanobiphenyl) doped with a small amount (typically 1% by weight) of a chiral molecule such as R811 [R-(+)-octan-2-yl 4-(4-(hexyloxy)benzoyl) benzoate], the freezing range is usually very small (typically of the order of 0.02 °C). However, it is possible to increase considerably the freezing range by doping the cholesteric phase with an impurity. This makes easier the observation of the cholesteric droplets coexisting with their isotropic liquid. In 1900, Lehmann observed that these droplets are not static but rotate constantly when they are submitted to a temperature gradient [2]. This phenomenon was then re-observed by one of us (P.O.) and A. Dequidt in 2008 [3,4] and more recently by other authors [5–7]. The first explanation of this phenomenon was given by Leslie in 1968 [8]. According to Leslie, a cholesteric phase subjected to a temperature gradient $\vec{G}$ experiences a torque of expression:

$$\vec{\Gamma}_{TM} = \nu \vec{n} \times (\vec{n} \times \vec{G}), \tag{1}$$

where ν is the Leslie thermomechanical coefficient [9]. It turns out that this torque exists and has been measured experimentally, first in a compensated cholesteric LC [10–12] and then in diluted cholesteric LCs [13]. However, this torque is too small by several orders of magnitude—with sometimes the bad sign—to explain the Lehmann rotation of the droplets [13–15]. The same conclusion was drawn for the Lehmann rotation of twisted nematic droplets observed recently in a chromonic LC [16]. In that case, a similar explanation based on the existence of a thermomechanical torque proportional to the twist of the director field (the so-called Akopyan and Zel'dovich torque [17,18]) was first proposed [16] but rapidly invalidated after this torque was measured experimentally [19,20].

The main conclusion of these previous works is that the Leslie and (or) Akopyan and Zel'dovich thermomecanical terms cannot explain the Lehmann rotation of the cholesteric and nematic droplets (when the later are twisted). Another explanation must thus be found. One of them was recently suggested by Bono *et al.* [21] who observed a reversal of the sense of rotation of the cholesteric droplets when the sample, initially doped with an azobenzene, is irradiated with UV light. To explain this spectacular effect, these authors show the existence of two permanent crossed fluxes of the *cis* and *trans* isomers of the azobenzene across the droplets that are driven by the UV light. These fluxes of matter induce a torque on the director that is formally equivalent to the thermomechanical torque of Leslie. The existence of this torque was first predicted by de Gennes in his book on liquid crystals [22] and was then experimentally observed in chiral Langmuir monolayers [23–25], in smectic C* free-standing films [26], and in thin shells of cholesteric LC [27].

The question we are asking in this paper is thus the following: is the Lehmann effect due to a chemical effect, or more precisely due to a flux of impurities across the droplets? To answer this question, we adopt a four-stage approach. First we show that there must exist a flux of impurities across the droplets (Sec. II). Then we analyze experimentally whether this flux can explain the Lehmann effect (Sec. III). Finally, we reanalyze the experiment of Bono *et al.* [21] in the light of our results (Sec. IV) before concluding by proposing new avenues of reflection to understand the Lehmann effect (Sec. V).

*patrick.oswald@ens-lyon.fr

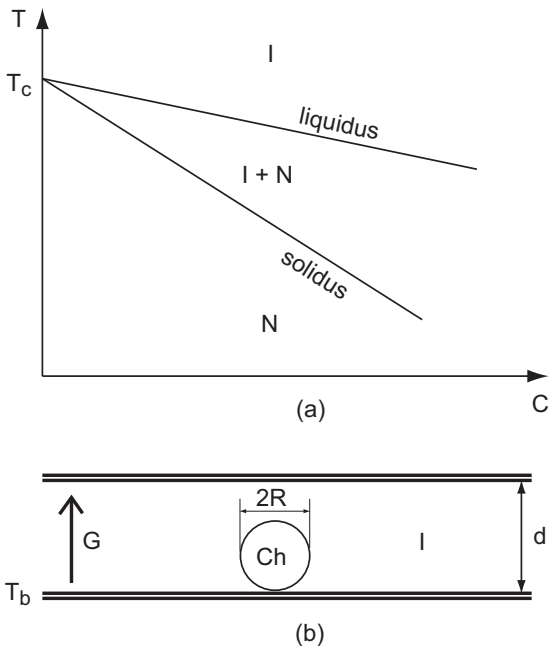

FIG. 1. (a) Typical phase diagram in the diluted regime. The slope of the liquidus is m (here negative) and the slope of the solidus is m/K; (b) droplet in the sample when the two phases coexist.

II. ON THE SPHERICAL SHAPE OF THE CHOLESTERIC DROPLETS

There is much experimental evidence that the cholesteric droplets are spherical when they coexist with their isotropic liquid and their diameter is smaller than the sample thickness. This result was obtained by various techniques including direct imaging with a confocal microscope [5] and indirect shape determination via the measurement of their optical transmittance in the polarizing microscope [28]. This shape is easily predicted when the sample is maintained at constant temperature in the coexistence region between the two phases because it is the shape that minimizes the surface energy (by assuming a constant surface tension). However, the determination of the shape is more complex when the sample is subjected to a temperature gradient. In this case, the droplet must locally satisfy the Gibbs-Thomson relation between the interface temperature T, the interface curvature κ, and the impurity concentration at the interface in the isotropic liquid C_{iI} (with index i standing for "interface" and index I for "isotropic") [1]

$$T = T_c - \frac{\gamma T_c}{\Delta H}\kappa + mC_{iI}. \tag{2}$$

In this equation, T_c is the melting temperature of the pure cholesteric phase, m is the slope of the liquidus (a straight line at small concentration of impurities, see Fig. 1), ΔH is the latent heat per unit volume, and γ is the surface tension taken constant for simplicity. For completeness, we recall the expression of κ for a surface of revolution obtained by rotating a curve of equation $x = x(s)$, $z = z(s)$ in the xz plane about the z axis (with s the arclength):

$$\kappa = \frac{1}{x}\frac{dz}{ds} - \frac{dz}{ds}\frac{d^2x}{ds^2} + \frac{dx}{ds}\frac{d^2z}{ds^2}, \tag{3}$$

with the constraint

$$\left(\frac{dx}{ds}\right)^2 + \left(\frac{dz}{ds}\right)^2 = 1. \tag{4}$$

Note that in Eq. (2), we neglected the elastic corrections due the deformations of the director field. These corrective terms, of the form $\frac{T_c\bar{K}}{\Delta H R_C^2}$, where $1/R_C$ is the so-called molecular orientation curvature at the interface [1,29] and $\bar{K}$ is a Frank constant, are indeed completely negligible as long as $R_C >$ 100 nm, which is the case in the banded droplets studied experimentally in this paper (see the next section).

This differential equation gives the shape of the droplets provided that the wetting conditions on the plates are specified. In practice, the plates are treated with a polymer so that the cholesteric phase dewets. In this condition, this equation can be solved if the concentration and the temperature at the interface are known. The temperature field is easily found if one assumes that the two phases have the same thermal conductivity. In that case $T = T_b + Gz$, where z is the vertical coordinate and T_b is the temperature of the bottom cold plate (Fig. 1). For the concentration field, the situation is much more complex because one must solve the diffusion equations for the concentration fields in the two phases. This is a difficult task that cannot be done simply, in particular when the boundary of the droplet is not known (free-boundary problem well known from people working in crystal growth).

However, a solution exists if one assumes that the impurity concentration in the isotropic phase C_I and that C_N in the nematic phase are constant, with $C_N = KC_I$, where K is the partition coefficient of the impurity (see Fig. 1). Under this assumption, the diffusion equations are automatically satisfied as well as the law of conservation of the impurities at the interface because of the absence of fluxes in the two phases. As for the global conservation of impurity in the sample, it can be satisfied by fixing the volume V of every droplet and their number n per unit volume so that $nVC_N + (1 - nV)C_I = \bar{C}$, where $\bar{C}$ is the average concentration of impurity in the sample. Under these assumptions, it can be shown that the shape of the droplets depends on their relative size with respect to the typical length $L = \sqrt{L_c L_T}$ where $L_c = \gamma/\Delta H$ is the capillary length and $L_T = T_c/G$ is the thermal length. More precisely, the droplets have an almost spherical shape if their radius $R < L$ and a flat shape as shown in Fig. 2 when $R > L$. In the later case, the height of the droplet saturates and cannot exceed $\sim 2L$. This flattening is due to the temperature gradient and is similar to the one observed with a drop of water on a substrate in the gravity field (in this case L is replaced by the gravitational length).

It turns out that these predictions are not at all satisfied experimentally. Indeed, let us estimate the length L. According to previous measurements, $\Delta H \approx 10^6$ J/m^3 [30] and $\gamma \approx 10^{-5}$N/m [31,32]. This gives an extremely small capillary length $L_c \approx 10^{-11}$ $m = 0.1$ Å. In a typical experiment (see below), $G \approx 2\ 10^4$ K/m and $T_c \approx 300$ K, which gives $L_T \approx 0.015$ m. As a consequence, $L \approx 4\ 10^{-7}$ m $= 0.4$ μm. This is very small, much smaller than the radius of the usual droplets observed in the experiments on the Lehmann effect. This strong disagreement shows that the surface tension is not large enough to oppose the flattening effect of the temperature

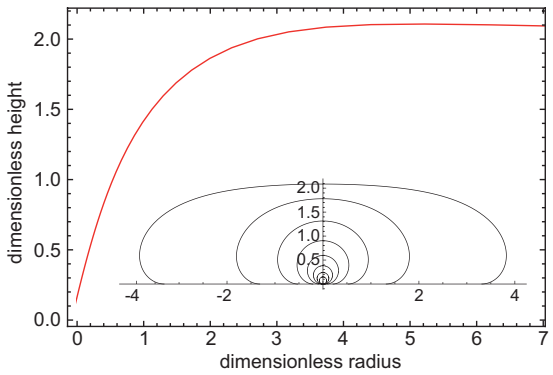

FIG. 2. Height and shape of the droplets as a function of their radius calculated by solving numerically the Gibbs-Thomson equation at equilibrium. The lengths are given in unit of $L = \sqrt{L_c L_T}$.

gradient. This result remains globally unchanged if the anisotropy of the surface tension and the elastic effects are taken into account, their only effect being to change a little the shape of the droplets.

The direct consequence of this calculation is that the spherical droplets observed experimentally are very different from the droplets "at equilibrium" [33] that we have just calculated. This shows that the droplets are dynamical in nature and result from an out-of-equilibrium growth process in the coexistence zone. This conclusion is reinforced by the observation that the droplets have a finite lifetime and are rarely stable over more than a few periods of revolution when they are polydisperse in size. The situation is different when they are monodisperse as in Fig. 4. In that case, they can survive much longer (tens of minutes) before disappearing or merging with a neighbor. This calculation also shows that, for the droplets observed in the Lehmann effect, the surface tension effects can be neglected in the Gibbs-Thomson relation, which becomes simply

$$T = T_c + mC_{iI} = T_b + Gz, \tag{5}$$

by assuming that the temperature gradient is the same everywhere (this is true if the two phases have the same thermal conductivity). This relation immediately shows that C_{iI} is a linear function of z. Because $C_{iN} = KC_{iI}$, we deduce that there must exist a gradient of impurity concentration inside the droplets of the order of

$$\nabla C_N \approx K\,\frac{G}{m}. \tag{6}$$

This result is obviously very approximate because a linear concentration profile of impurity does not satisfy the anisotropic diffusion equation in the droplet. In addition, we do not know how to calculate the concentration field in the liquid which satisfies the diffusion equation and the law of impurity conservation on the glass plates and the surface of the droplet. This is nonetheless not very important for our purpose because we only need the concentration field inside the droplet. In the following, we will therefore just admit that there exists a gradient of impurity concentration in the droplet given by Eq. (6).

Doing this, we can now reproduce the same model as in Ref. [3] by replacing the thermal Leslie torque by the chemical Leslie torque,

$$\vec{\Gamma}_{CM} = \nu_C \vec{n} \times (\vec{n} \times \vec{\nabla} C_N), \tag{7}$$

where ν_C is a chemical Leslie coefficient. At small concentration $C^\star$ of chiral molecule (diluted cholesteric), ν_C and the equilibrium twist q_0 must be proportional to $C^\star$ as these two quantities vanish for symmetry reason at $C^\star = 0$. As a consequence, ν_C must be proportional to q_0 and can written in the form $\nu_C = \bar{\nu}_C q_0$ where $\bar{\nu}_C$ only depends on the chemical nature of the impurity that diffuses across the droplet. From this modified model, we predict that the rotation velocity ω of the droplets must be of the form

$$\omega = -\Gamma \frac{\bar{\nu}_C}{mK}\,\frac{q_0 G}{\gamma_1}, \tag{8}$$

where γ_1 is the rotational viscosity and Γ a dimensionless positive function that—for a given texture of the droplets (banded droplets in our experiments)—only depends on the product $q_0 R$ by denoting by R the radius of the droplets. We recall that this model is based on the assumption that the rotation of the droplets is due to the only rotation of the director without flow, which was experimentally checked [34,35].

An important prediction of this model is that the rotation velocity of the droplets should not depend on the concentration of impurity, but only on the temperature gradient. This is true provided that m is constant, which imposes to work at small concentration of impurity, in the diluted regime. However, the rotation velocity must depend on the choice of the impurity because the physical constants $\bar{\nu}_C$, K, and m, and consequently the ratio $\bar{\nu}_C/(mK)$, must depend on it. In the next section we test this new version of the model.

III. EXPERIMENTAL VERIFICATION OF THE MODEL

To test these predictions, we doped a cholesteric LC with four different impurities. The LC chosen was the 7CB (from Frinton Laboratories, Inc., USA) and the chiral dopant was the R811 (from Merck, Germany). The impurities chosen were the biphenyl (from Sigma-Aldrich, Germany), the hexachoroethane (from Sigma-Aldrich, Germany), and a fluorinated polyether polymer (Polyfox PF-656 from Omnova Solutions, France), which are nonmesogenic, and the LC I52 (4-ethyl-2- fluoro-4 -[2-(trans-4-pentylcyclohexyl)-ethyl] biphenyl from Merck, Germany), which is mesogenic and has a nematic phase between 24 and 103.4 °C [36]. The phase diagrams of 7CB doped with these impurities are shown in Fig. 3. The corresponding values of the slope of the liquidus and the partition coefficient are given in Table I. We emphasize that the slope of the liquidus is negative for all the nonmesogenic impurities and positive for the LC I52.

For the liquid polymer Polyfox PF-656, we were not able to determine the exact phase diagram, because this impurity is very little soluble in 7CB. In practice, we mixed 7CB with 5 wt.% of Polyfox. This mixture was then vigorously stirred and centrifuged at 25 °C to separate the polyfox-rich phase (of density close to 1.27) from the 7CB-rich phase (of density close to 1). For this sample of 7CB saturated in Polyfox, we measured $T_{\text{solidus}} = 39.69\,^\circ\text{C}$ and $T_{\text{liquidus}} = 40.20\,^\circ\text{C}$, which gives $K = 0.73$ by taking $T_c = 41.59\,^\circ\text{C}$ for the pure 7CB

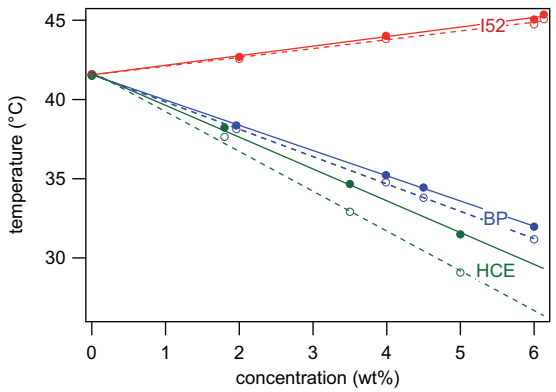

FIG. 3. Phase diagrams in the diluted regime of the LC 7CB doped with impurities I52, BP (biphenyl) and HCE (hexacholorethane). The solidus (liquidus) lines are shown in dashed (solid) line. For the pure 7CB we measured a freezing range of the order of 0.01 °C. This could be due to the presence of traces of water which is the main impurity in biphenyl LCs.

and by assuming that the solidus and liquidus lines are still straight lines. By contrast, we could not determine the slope of the liquidus because the real concentration of Polyfox is unknown. This is the reason why the phase diagram with the Polyfox is not shown in Fig. 3.

Each mixture of 7CB doped with its impurity was then doped with the chiral dopant R811 (from Merck, Germany). In all experiments, the concentration by weight of R811 was taken equal to 1.27%. The composition of the different mixtures used in these experiments is given in Table II. We emphasize that with this concentration of R811 the phase diagrams shown in Fig. 3 are just shifted downwards by $\sim 0.76\,^{\circ}\mathrm{C}$ without notable change of the slopes of the liquidus and solidus lines. This is due to the fact that the partition coefficient of R811 is close to 1 in biphenyl LCs [37]. For each mixture, we additionally measured the cholesteric pitch P (or equivalently the equilibrium twist $q_0 = 2\pi/P$) at the solidus temperature by using the Cano-wedge method [1]. The viscosity γ_1 was also measured at the solidus temperature in the nematic phase (before introduction of the R811) by using the Freedericksz transition following the method described by Wu and Wu [38]. The values of q_0 and γ_1 are reported in Table II for all the samples used. We found that the equilibrium twist was almost the same in all the samples at the solidus temperature, of the order of 0.935 $\mu\mathrm{m}^{-1}$. By contrast, the viscosity significantly changed from one sample to another, from 0.021 Pa s in the sample doped with 6.17 wt.% of I52 to 0.0305 Pa s in the sample doped with 5 wt.% of HCE.

TABLE I. Slope of the liquidus m and partition coefficient K of the impurities used in this work.

Impurity	Liquidus slope (K/wt%)	Partition coefficient
BP	−1.59	0.92
HCE	−2.01	0.80
PF-656	–	0.73
I52	0.60	1.09

TABLE II. Mixtures used to measure the Lehmann effect and their physical properties. The viscosity γ_1 has been measured in the nematic phase. In all the mixtures, the concentration of R811 was chosen equal to 1.27% by weight. In sample 7, the undissolved PF-656 was separated from the LC by centrifugation after a strong stirring at 25 °C.

Impurity	Mixture no.	Conc. (wt.%)	q_0 ($10^6\mathrm{m}^{-1}$)	γ_1 (Pa s)
Pure 7CB	1	0	0.934	0.0215
BP	2	0.997	0.934	0.0220
BP	3	1.99	0.935	0.0228
BP	4	2.99	0.937	0.0240
BP	5	3.97	0.938	0.0245
BP	6	4.75	0.939	0.0253
HCE	7	5.00	0.939	0.0305
PF-656	8	Saturated (25 °C)	0.934	0.0243
I52	9	6.17	0.935	0.0210

The measurements of the rotation velocity of the texture of the cholesteric droplets were performed by using 20-μm-thick samples. All the samples were sealed with the UV glue NOA 81 (from Norland Products Inc., USA) to avoid that the impurity evaporates from the edges. This is particularly important with the biphenyl as was shown in Ref. [39] and with the hexachloroethane, which evaporates even faster than the biphenyl. The two glass plates limiting the samples were covered with a thin layer of polymercaptan (typical thickness 50–100 nm) following the method described in Ref. [40]. With this surface treatment, the cholesteric droplets systematically dewet the surface which improves the reproducibility of the measurements. In practice, the polymercaptan dissolves a little in the LC and systematically decreases the liquidus and solidus temperatures of about 0.3 and 0.6 °C, respectively. The experimental setup used to impose the temperature gradient is described in Ref. [3]. In all of our experiments the temperature difference between the two ovens ΔT ranged between 5 and 10 °C. This gives a temperature gradient in the sample of the order of 1700 ΔT (K/m) by taking a ratio between the thermal conductivity of the glass and that of the LC of the order of 7 [41]. All measurements were performed with the banded droplets, in which the helical axis is perpendicular to the temperature gradient (Fig. 4). These droplets are by far the most numerous in the samples, even if one sometimes observed other types of droplets as the ones with a low contrast visible in Fig. 4. These droplets rotate faster than the others, but we did not study them because they were only observed in the samples doped with the polyfox and the HCE. In the following, Θ is the period of rotation of the banded droplets, R is their radius, and ΔT is the imposed temperature difference between the two ovens.

The data for mixtures 2–6 with different concentrations of biphenyl are shown in Fig. 5. In this figure, we plotted the combination $q_0 \Delta T \Theta/\gamma_1$ as a function of the dimensionless product $q_0 R$. As we can see, all the curves fall on the same master curve. This agrees with Eq. (8) of the chemical model that predicts that this quantity must be an universal function of $q_0 R$. Note that in this graph, we added the results obtained with the pure cholesteric phase which surprisingly, also fall on the same master curve. In this case, the main impurity is not

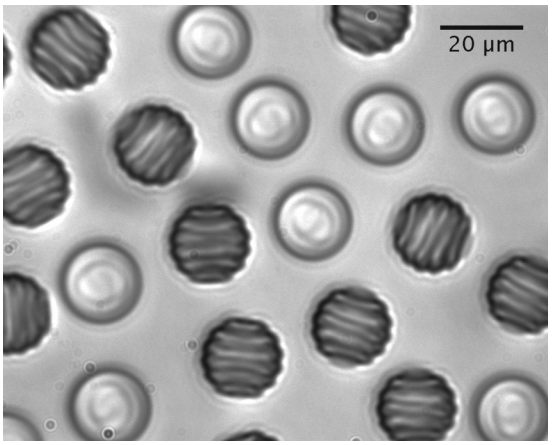

FIG. 4. Two types of cholesteric droplets coexisting with the isotropic liquid. All the droplets rotate clockwise when the temperature gradient is directed towards the reader. Only the rotation of the banded droplets has been studied. For information, the droplets with the low contrast rotate typically 11 times faster than the banded droplets in this sample of the mixture 7CB + 1.27%R811+ 5%PF-256.

the biphenyl but the polymercaptan dissolved in the LC. This suggests that the chemical nature of the impurity does not play a dominant role in the Lehmann rotation.

To test this point, we performed similar measurements with samples 7–9 doped this time with HCE, PF-656, and I52,

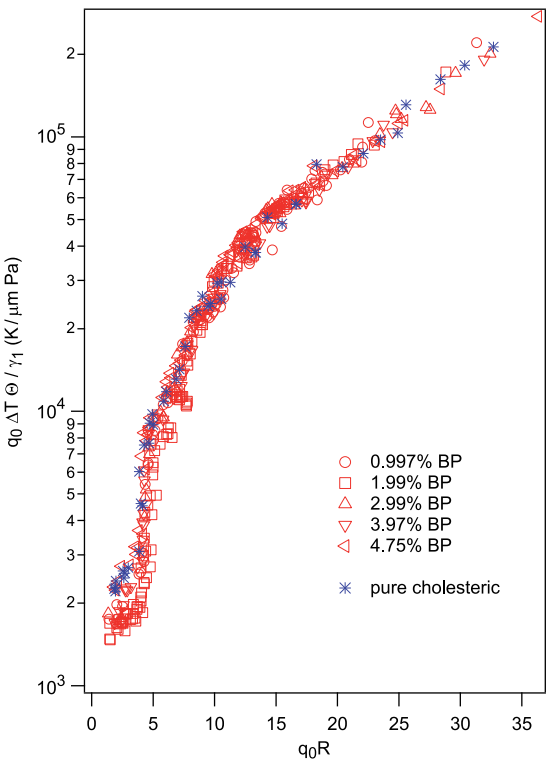

FIG. 5. Experimental data obtained with the samples doped with the biphenyl. By way of comparison, the data obtained with the pure cholesteric phase are also shown in this graph. In all these experiments, the glass plates were treated with the polymercaptan.

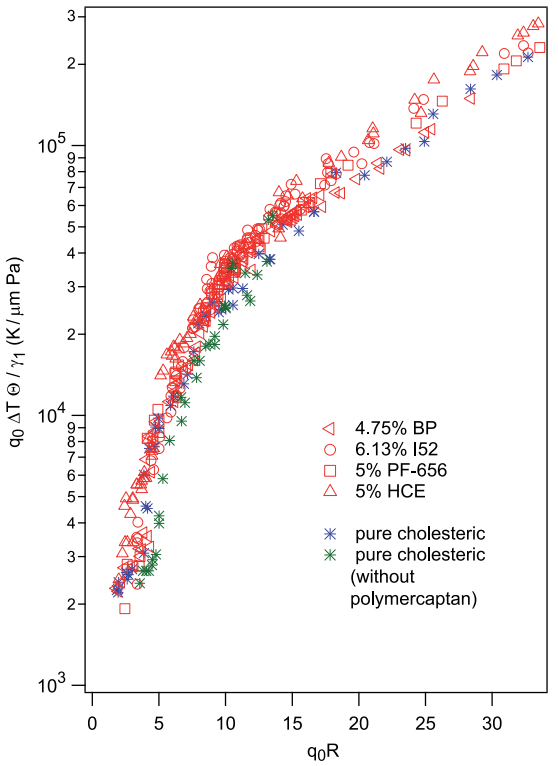

FIG. 6. Comparison between the experimental data for samples doped with different impurities. In all these experiments, the glass plates were treated with the polymercaptan. Only the green stars have been measured in a sample without polymercaptan. In this case, the data were more dispersed and only the droplets that were freely rotating were measured.

respectively. Again, we found that all the curves fall on the same master curve (Fig. 6). This is indeed not expected from the model because the factor $\bar{\nu}_C/(mK)$ in Eq. (8) should clearly depend on the impurity if the rotation was due to a chemical Leslie torque. In addition, we observed that the droplets rotate in the same direction in all the samples, regardless of the sign of m. This would mean that the Leslie coefficient has the same sign as m, which would be surprising. One possibility suggested by one of the referees to explain these observations would be that the rotation is dominated by the flux of polymercaptan present in all the samples. To test this assumption, we prepared a sample of pure cholesteric without the polymercaptan layers and found that the droplets were rotating with the same velocity as before. Points obtained in this way are shown in Fig. 6 (green stars). This proves that the polymercaptan is not directly responsible for the rotation of the droplets. The same conclusion holds for the chiral molecule R811 which acts also as an impurity, because it has been shown previously that the rotation velocity of the droplets is independent of the nature of the chiral molecule provided that the pitch is the same [42].

Finally, we emphasize that the scaling proposed in Figs. 5 and 6 only works if γ_1 is taken into account. This proves that the rotation velocity of the banded droplets is inversely proportional to γ_1, which supports the idea that the rotation of the droplets involves a rotation of the director without flow.

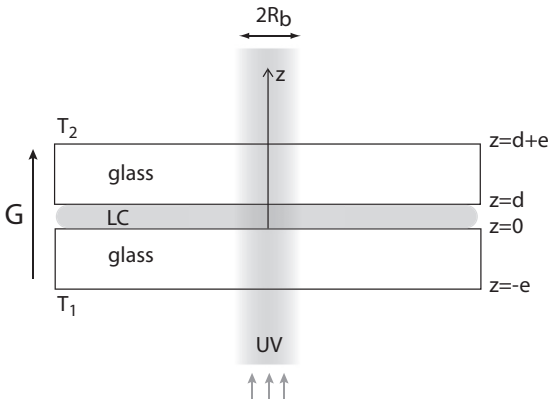

FIG. 7. Geometry of the experiment.

From these results, we conclude that the Lehmann rotation is certainly not driven by a chemical Leslie torque. This led us to re-analyze the experiment of Bono *et al.* [21].

IV. ABOUT THE EXPERIMENT BY BONO *ET AL.* ON THE ROTATION OF CHOLESTERIC DROPLETS DRIVEN BY UV-LIGHT IRRADIATION

Recently, Bono *et al.* [21] investigated the Lehmann effect in a cholesteric sample doped with an azobenzene molecule. In their experiment, the sample was submitted to a constant temperature gradient and was simultaneously illuminated by a UV-beam of variable intensity. By doing this, they observed that the rotation velocity of their droplets could vanish and change sign when the intensity of the beam was increased. This spectacular reversal of the sense of rotation of the droplets was interpreted as due to the appearance of two crossed fluxes of the *trans* and *cis* isomers of the azobenzene across the droplets. According to the authors these two fluxes generate two chemical Leslie torques which add to the usual Lehmann torque due to the imposed temperature gradient. This interpretation is tempting on condition that the temperature gradient in the sample is not significantly changed, which is what the authors claimed after they roughly estimate the temperature increase of their sample under UV (of the order of 0.01 °C at the critical intensity at which the reversal is observed, which is indeed completely negligible).

In this section, we reconsider this estimate by performing a numerical simulation of the thermal problem in the experimental conditions of Bono *et al.* To calculate the temperature field in the sample, we need to solve the heat diffusion equation in both the LC sample and the glass plates, with the adequate boundary conditions. The geometry of the problem is described in Fig. 7. In the glass plates, the heat diffusion equation simply reads

$$\mathrm{div}\,\vec{j} = 0 \quad \text{with} \quad \vec{j} = -\kappa_g \overrightarrow{\mathrm{grad}}\, T, \tag{9}$$

where κ_g is the thermal conductivity of the glass. In the LC, this equation reads

$$\mathrm{div}\,\vec{j} - P = 0 \quad \text{with} \quad \vec{j} = -\kappa_{\mathrm{LC}} \overrightarrow{\mathrm{grad}}\, T, \tag{10}$$

where κ_{LC} is the thermal conductivity of the LC (supposed to be constant and the same in the two phases for simplicity) and P is a source of heat of the form

$$P = -\frac{dI}{dz} \tag{11}$$

by denoting by $I(z,r)$ the intensity in polar coordinates of the UV beam. For a circular Gaussian beam of radius R_b, the Lambert law gives

$$I(r,z) = I_0 \exp(-\alpha z) \exp\left(-\frac{r^2}{R_b^2}\right). \tag{12}$$

At the two interfaces between the glass plates and the LC the flux of heat must be conserved, which imposes

$$\vec{j}_g \cdot \vec{z} = \vec{j}_{\mathrm{LC}} \cdot \vec{z} \quad \text{at} \quad z = 0 \quad \text{and} \quad z = d. \tag{13}$$

Finally, the temperatures are imposed on the outer faces of the glass plates:

$$T(z = -e) = T_1 \quad \text{and} \quad T(z = d + e) = T_2 \tag{14}$$

by denoting by e (d) the thickness of the glass plates (the sample).

This set of equations was solved with Mathematica by using a finite-element method. In the calculation, we chose $T_1 = 65\,^{\circ}\mathrm{C}$, $T_2 = 70\,^{\circ}\mathrm{C}$ (which gives a typical gradient of $0.016\,^{\circ}\mathrm{C}/\mu\mathrm{m}$ in the sample), $e = 1$ mm, $d = 50\ \mu$m, $\kappa_g = 1$ mW mm^{-1} K^{-1}, $\kappa_{\mathrm{LC}}/\kappa_g = 1/7$, $R_b = 0.2$ mm, $\alpha = 0.45$ mm^{-1}, and $I_0 = 50$ mW/mm^2 (typical values given in Ref. [21]). The temperature profiles across the sample and the glass plates are shown in Fig. 8 as a function of the distance to the center of the beam. The bottom profile is the undisturbed profile observed far from the beam. As expected it is linear in both the glass plates and the LC with a slope ratio of 1/7 given by the ratio of the thermal conductivities. However, this profile considerably changes inside the beam and shifts towards the high temperatures because of the heating due to the absorption of the UV light. Still more interesting, the local temperature gradient can even change sign in the upper part of the sample. This could explain the reversal of the sense of rotation of the droplets present in this region. It is not clear at this stage of the discussion to know whether these thermal effects are responsible for the observations of Bono *et al.*, but our calculations show that the thermal effects are important in their experiment and cannot be neglected.

V. CONCLUSION: TOWARD AN ALTERNATIVE MODEL

In conclusion, our analysis reveals that the spherical droplets usually observed in the coexistence region are out of equilibrium—in the sense that they do not result from the simple minimization of their surface energy—when a temperature gradient is applied. Indeed, the only way to satisfy the Gibbs-thomson relation is to admit that there is a gradient of impurity across the droplets since the capillary term becomes negligible as long as their radius exceeds a few micrometers. This suggests that the spherical shape of the droplets is a growth shape rather than an equilibrium shape.

Based on this observation, we proposed that this gradient of impurity generates a flux of impurity responsible for a chemical Leslie torque on the director and we reformulated

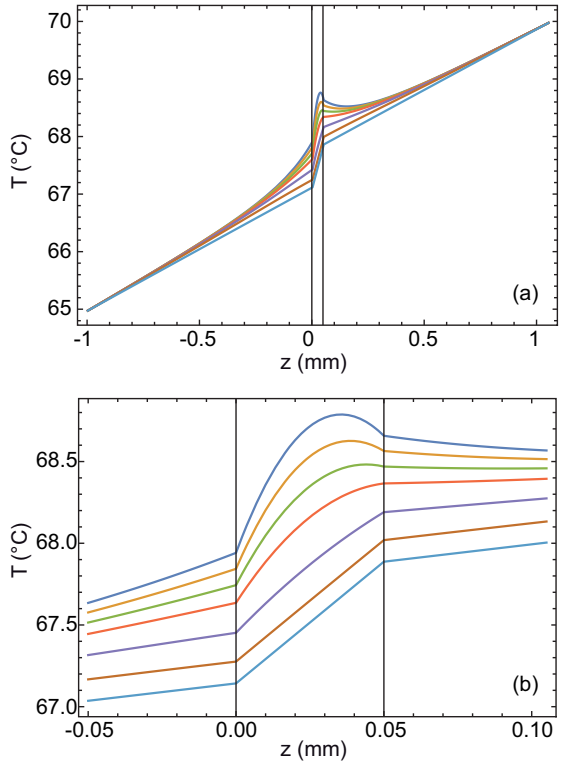

FIG. 8. (a) Temperature profiles numerically calculated across the LC sample and the glass plates at different distances from the center of the UV beam; (b) Zoom in the LC sample. From top to bottom $r = 0, 0.1, 0.15, 0.2, 0.3, 0.5$, and 2 mm. The two vertical bars mark the limits of the LC sample.

our old model of the Lehmann effect by replacing the thermal Leslie torque by the chemical Leslie torque. The surprising result of our experiments is that this torque—if it exists—is independent of the nature of the impurity. In addition, its sign should not depend on the sign of the slope of the liquidus, and thus on the sense in which the impurity diffuses. These two results are very suspicious and suggest that the Leslie chemical effect is not directly responsible for the Lehmann effect. The same conclusion could apply to the work of Bono *et al.*, in which the thermal effects are clearly underestimated.

However, we believe that the Lehmann effect is closely linked to the problem of the diffusion of the impurity across the droplets when a temperature gradient is applied. Indeed, this flux, as well as the Lehmann effect, only appears when the droplets are prepared in the coexistence region with their own isotropic liquid. This was recognized by several authors [7,16] who prepared dispersions of cholesteric droplets in immiscible—or very slightly miscible liquids such as water or glycerol—and never observed the Lehmann effect when the temperature was lower than the transition temperature of the LC in the droplets. In this case, the cholesteric phase is saturated with the liquid (for water, for instance, the saturation concentration is of the order of 0.6 wt% [43]) and the concentration gradient disappears. The shape of the droplet then just results from the minimization of the surface energy and the spherical shape is recovered (if one neglects the temperature variation of the surface tension and the flattening due to the

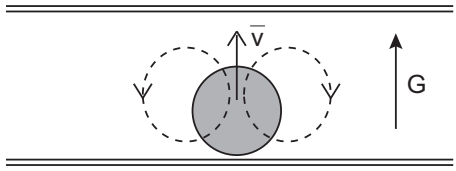

FIG. 9. Possible hydrodynamic flow in the presence of a droplet. The droplet keeps its stationary shape if the cholesteric phase melts at the top of the droplet and grows at the bottom. Because of this vertical motion the chiral internal texture of the droplet must rotate. Note that this flow is undetectable with the photobleaching technique used in Refs. [34,35] that is only sensitive to the flow in the plane of the sample.

gravity and the difference in density between the liquid and the LC). Note that in that case the surface tension is much larger than at the interface with the isotropic phase of the LC (of the order of 0.1 N/m [44] instead of the 10^{-5} N/m reported before), which favors the spherical shape. This difference of behavior between the droplets in the coexistence region and the droplets in an emulsion argues in favor of an important role played by the diffusion of impurities in the Lehmann effect.

For this reason, we tried to deepen our analysis in this direction by considering which other consequence the presence of a gradient of impurity implies. A new clue is given by applying the law of impurity conservation at the surface of the droplet:

$$C_{Ii}(1-K)\vec{v}\cdot\vec{\nu} = -D_I(\vec{\nabla}C)_I\cdot\vec{\nu} + D_{\rm Ch}(\vec{\nabla}C)_{\rm Ch}\cdot\vec{\nu}, \quad (15)$$

where $\vec{\nu}$ denotes the unit vector normal to the interface and directed from the cholesteric towards the isotropic liquid and $\vec{v}$ the growth velocity of the cholesteric phase. This equation shows that the quantity of solute which is rejected at the interface per unit time and surface is balanced by the diffusion currents in the two phases. If there is no flow in the sample and the droplet has a stationary shape as in Fig. 4, we have necessarily $\vec{v} = 0$ which means that the two fluxes must equilibrate. This seems impossible to satisfy except if there is a vertical flow which drags at velocity $\bar{v}$ the droplet in the opposite direction as shown schematically in Fig. 9. To estimate this velocity let us apply the previous equation at the top of the droplet. If this point is close to the top glass plate, one should have

$$D_I(\vec{\nabla}C)_I\cdot\vec{\nu} \approx 0, \quad (16)$$

because there is no flux of impurity across the glass plate. By contrast, one has

$$D_{\rm Ch}(\vec{\nabla}C)_{\rm Ch}\cdot\vec{\nu} \sim K D_{\rm Ch}\frac{G}{m}, \quad (17)$$

according to Eq. (6), which gives

$$\bar{v} = -v \sim -K D_{\rm Ch}\frac{G}{mC_{Ii}(1-K)}, \quad (18)$$

where C_{Ii} must be of the order of the average concentration $\bar{C}$ of impurity. This vertical motion of the droplet leads to an apparent rotation of its internal texture at angular velocity

$$\omega \sim -q\bar{v} = qKD_{\rm Ch}\frac{G}{m\bar{C}(1-K)}, \quad (19)$$

where q is the twist of the droplet in the vertical direction (proportional to q_0). This formula is interesting in many respects.

First, it predicts the good sense of rotation of the droplet whatever the impurity chosen. Indeed, the experiment shows that in all cases $\omega < 0$ when $q_0 > 0$. This is the case for nonmesogen impurities for which $m < 0$ and $K < 1$ but also for the nematogen impurity I52 for which $m > 0$ and $K > 1$;

Second, it predicts that ω is proportional to G, which is observed in all experiments.

Third, it predicts that ω is proportional to the effective twist in the z direction. This is compatible with experiments that show that the CC (for concentric-circles) droplets in which the helix is parallel to the temperature gradient rotate much faster than the banded droplets in which the twist is mainly in the direction perpendicular to the gradient. More precisely this formula predicts that the more tilted the helical axis with respect to the temperature gradient, the smaller must be the rotation velocity. This tendency was indeed observed experimentally by the authors of Ref. [5]. It must be emphasized here that the banded droplets never stop rotating in spite of the fact that the helical axis is perpendicular to the temperature gradient in the center of the droplets. The reason is that these droplets always exhibit double twist near their surfaces, as shown both theoretically and experimentally by confocal microscopy in Ref. [6]. This result was confirmed numerically in Ref. [28]. This particular structure induces a rotation of the edge of the droplets that extends to the whole texture because of the nematic elasticity. For this reason, the molecules must also rotate—and not only translate—inside these droplets. This molecular rotation induces a strong energy dissipation very similar to the one described in the standard model based on the Leslie torque [3,4]. This could qualitatively explain why the rotation velocity of the banded droplets depends on γ_1 and strongly decreases when their diameter increases. By contrast, the rotation velocity of the CC droplets must be independent of their diameter in this model, since no molecular rotation is necessary to observe the texture rotation. This was indeed observed by Ito *et al.* [6] in their experiments.

Fourth, it predicts the good order of magnitude for the rotation velocity of the droplets. To check this point, we can rewrite Eq. (19) in the form

$$\Theta q \Delta T = \frac{2\pi \delta T}{D_{\mathrm{Ch}} a}, \tag{20}$$

where ΔT is the imposed temperature difference (with $G = a\Delta T$ and $a = 1.7 \times 10^{-3}\ \mu\mathrm{m}^{-1}$) and $\delta T = m\bar{C}(K-1)/K$ is the freezing range. For CC droplet for which $q = q_0$, experiments show that their velocity is the same as the one measured for the banded droplet at very small radius [46]. By using this remark and the results of Fig. 5, we deduce that for CC droplets $\Theta q_0 \Delta T \approx 45$ K s $\mu\mathrm{m}^{-1}$ by taking $\gamma_1 \approx 0.03$ Pa s while the previous formula predicts $\Theta q_0 \Delta T \approx 70$ K s $\mu\mathrm{m}^{-1}$ by taking $\delta T = 1\,^{\circ}\mathrm{C}$ and $D_{\mathrm{chol}} = 50\ \mu\mathrm{m}^2\mathrm{s}^{-1}$ (see Table III).

However, Eq. (20) suggests that the period of rotation increases when the freezing range increases, which is not observed. It thus becomes obvious that this oversimplified version of the model of melting-recrystallization is incomplete and must be improved.

TABLE III. Impurity diffusion coefficient perpendicular to the director measured in the nematic phase at the solidus temperature. The measurement was performed in directional melting with homeotropic samples (for more details, see Ref. [45]).

Impurity	$D_\perp$ ($\mu\mathrm{m}^2/s$)
BP	77
HCE	73
PF-656	30
I52	61

At this point we can mention that we have neglected the thermodiffusion (or Soret effect [47]) in our discussion. This phenomenon is rarely taken into account in crystal growth, but it could be important in liquid crystals, in particular inside the droplets where a spatial variation of the quadrupolar order parameter is imposed by the temperature gradient. This was evidenced in a recent experiment showing the spontaneous migration of a fluorescent dye in a zone heated by a laser focused on the sample [48]. In this experiment the concentration and temperature gradients are of the same sign at equilibrium, which means that the thermodiffusion coefficient of the dye is negative. This is expected if the dye prefers the isotropic liquid as the nonmesogenic impurities used in this study for which $m < 0$ and $K < 1$. Conversely, we could expect a positive thermodiffusion coefficient for the I52 impurity for which $m > 0$ and $K > 1$. If we are right, we thus predict gradients of impurity concentration which are of the same sign as the temperature gradient for the nonmesogenic impurities (BP, HCE, polyfox, and polymercaptan) and of opposite signs for the I52. This is exactly the contrary of what we need to satisfy the Gibbs-Thomson equation. We thus conclude that the Soret effect is certainly negligible in our experiments since it should tend to flatten the droplets which is not observed.

In the future, it would be interesting to reconsider the model proposed in Ref. [49] and to generalize it by taking into account the mechanism of melting-recrystallisation proposed in this paper. This could be interesting because this model predicts that the period of rotation of the droplets is proportional to γ_1 and does not involve the thermal and chemical Leslie torques. This would require to solve first the problem of the nucleation and growth of the droplets in the presence of hydrodynamic flows, a nice challenge for theorists of crystal growth. This would be fundamental to understand the spherical shape of the droplets. From this resolution, the concentration field could be deduced and the rotation velocity calculated after correction of the vertical motion of the droplet. It would also be important to detect experimentally these vertical flows, for instance by improving the spatial resolution of the photobleaching experiments of Refs. [34,35], and to measure the variations of the elastic constants at the solidus temperature as a function of the concentration impurity, an essential ingredient in the model of Ref. [49].

The case of the Lehmann rotation of cholesteric droplets dispersed in the liquid polymer Polyfox PF-656—in which the LC is partly miscible—is also extremely interesting in light of our discussion [7]. Indeed, the surface tension between the

Polyfox and the LC must be much higher than in the present experiments because the chemical compositions of the two phases are very different. For this reason, the spherical shape of the droplets is less surprising and should simply result from the minimization of the surface energy of the droplets. However, the surface tension could vary significantly with temperature because of the partial miscibility between the LC and the Polyfox. In this case, one could imagine a strong Marangoni effect and a coupling between the induced flow and the cholesteric structure of the droplet similar to the one described recently by Yamamoto and Sano [50,51].

In conclusion, the Lehmann effect is far from being resolved, and could have different origins depending on the system considered. Among them are the thermal and chemical Leslie, Akopyan, and Zel'dovich torques, the melting-recrystallization process and the Marangoni effect. In our opinion, the thermal and chemical torques can always be neglected, except, perhaps in the experiment of Bono *et al.* [21], where a strong flux of azo dyes is generated under UV illumination. However, we favor the melting-recrystallization process in the classical Lehmann effect observed in the coexistence region between the cholesteric phase and its isotropic liquid and a Marangoni effect in the case of the cholesteric emulsions of Yoshioka and Araoka [7].

ACKNOWLEDGMENTS

The authors warmly thank A. Dequidt for his critical reading of the manuscript and very useful comments and suggestions, Dr. Werner Becker from Merck for the free sample of R811 and Dr. Stephane Dumas from Omnova Solutions for the free sample of Polyfox PF-656.

[1] P. Oswald and P. Pieranski, *Nematic and Cholesteric Liquid Crystals: Concepts and Physical Properties Illustrated by Experiments* (CRC Press, Boca Raton, 2005).

[2] O. Lehmann, Structur, system und magnetisches verhalten flüssiger krystalle und deren mischbarkeit mit festen, Ann. Phys. (Leipzig) **307**, 649 (2016).

[3] P. Oswald and A. Dequidt, Measurement of the Continuous Lehmann Rotation of Cholesteric Droplets Subjected to a Temperature Gradient, Phys. Rev. Lett. **100**, 217802 (2008).

[4] A. Dequidt, Effet lehmann dans les cristaux liquides cholestériques, Ph.D. thesis, No. d'ordre: 481 (2008).

[5] T. Yamamoto, M. Kuroda, and M. Sano, Three-dimensional analysis of thermomechanically rotating cholesteric liquid crystal droplets under a temperature gradient, Europhys. Lett. **109**, 46001 (2015).

[6] F. Ito, J. Yoshioka, and Y. Tabe, Heat-driven rotation in cholesteric droplets with a double twisted structure, J. Phys. Soc. Jpn. **85**, 114601 (2016).

[7] J. Yoshioka and F. Araoka, Topology-dependent self-structure mediation and efficient energy conversion in heat-flux-driven rotors of cholesteric droplets, Nat. Commun. **9**, 432 (2018).

[8] F. M. Leslie, Some thermal effects in cholesteric liquid crystals, Proc. R. Soc. London A **307**, 359 (1968).

[9] Strictly speaking, this coefficient also includes a "nematic" Akopyan and Zel'dovich correction proportional to q_0 [17,18] as was shown in Ref. [19].

[10] N. Éber and I. Jánossy, An experiment on the thermomechanical coupling in cholesterics, Mol. Cryst. Liq. Cryst., Lett. **72**, 233 (1982).

[11] A. Dequidt, A. Żywociński, and P. Oswald, Lehmann effect in a compensated cholesteric liquid crystal: Experimental evidence with fixed and gliding boundary conditions, Eur. Phys. J. E **25**, 277 (2008).

[12] P. Oswald and A. Dequidt, Direct measurement of the thermomechanical lehmann coefficient in a compensated cholesteric liquid crystal, Europhys. Lett. **83**, 16005 (2008).

[13] P. Oswald, Leslie thermomechanical power in diluted cholesteric liquid crystals, Europhys. Lett. **108**, 36001 (2014).

[14] P. Oswald, About the leslie explanation of the lehmann effect in cholesteric liquid crystals, Europhys. Lett. **97**, 36006 (2012).

[15] P. Oswald, Microscopic vs macroscopic origin of the lehmann effect in cholesteric liquid crystals, Eur. Phys. J. E **35**, 10 (2012).

[16] J. Ignés-Mullol, G. Poy, and P. Oswald, Continuous Rotation of Achiral Nematic Liquid Crystal Droplets Driven by Heat Flux, Phys. Rev. Lett. **117**, 057801 (2016).

[17] R. S. Akopyan and B. Y. Zel'dovich, Thermomechanical effects in deformed nematics, JETP **60**, 953 (1984).

[18] G. Poy and P. Oswald, On the existence of the thermomechanical terms of Akopyan and Zel'dovich in cholesteric liquid crystals, Liq. Cryst. **45**, 1428 (2018).

[19] P. Oswald, G. Poy, and A. Dequidt, Lehmann rotation of twisted bipolar cholesteric droplets: role of Leslie, Akopyan and Zel'dovich thermomechanical coupling terms of nematodynamics, Liq. Cryst. **44**, 969 (2016).

[20] G. Poy, Sur la pertinence du modèle thermomécanique dans la rotation lehmann des gouttes cholestériques et nématiques, Ph.D. thesis (2018).

[21] S. Bono, S. Sato, and Y. Tabe, Unidirectional rotation of cholesteric droplets driven by UV-light irradiation, Soft Matter **13**, 6569 (2017).

[22] P. G. de Gennes, *The Physics of Liquid Crystals* (Clarendon Press, Oxford, 1974).

[23] Y. Tabe and H. Yokoyama, Nat. Mater. **2**, 806 (2017).

[24] P. Milczarczyk-Piwowarczyk, A. Żywociński, K. Noworyta, and R. Hołyst, Collective rotations of ferroelectric liquid crystals at the air/water interface, Langmuir **24**, 12354 (2008).

[25] F. Bunel, J. Ignés Mullol, F. Saguès, and P. Oswald, Chemical leslie effect in Langmuir monolayers: A complete experimental characterization, Soft Matter **14**, 4835 (2018).

[26] K. Seki, K. Ueda, Y.-I. Okumura, and Y. Tabe, Nonequilibrium dynamics of 2D liquid crystals driven by transmembrane gas flow, J. Phys.: Condens. Matter **23**, 284114 (2011).

[27] A. Darmon, M. Benzaquen, S. Čopar, O. Dauchot, and T. Lopez-Leon, Topological defects in cholesteric liquid crystal shells, Soft Matter **12**, 9280 (2016).

[28] G. Poy, F. Bunel, and P. Oswald, Role of anchoring energy on the texture of cholesteric droplets: Finite-element simulations and experiments, Phys. Rev. E **96**, 012705 (2017).
[29] J. B. Fournier, Generalized Gibbs-Thomson Equation and Surface Stiffness for Materials with an Orientational Order Parameter, Phys. Rev. Lett. **75**, 854 (1995).
[30] G. Gray, K. J. Harrison, and J. A. Nash, New family of nematic liquid crystals for displays, Electron. Lett. **9**, 130 (1973).
[31] S. Faetti and V. Palleschi, Measurement of the interfacial tension between nematic and isotropic phase of some cyanobiphenyls, J. Chem. Phys. **81**, 6254 (1984).
[32] P. Oswald and G. Poy, Droplet relaxation in Hele-Shaw geometry: Application to the measurement of the nematic-isotropic surface tension, Phys. Rev. E **92**, 062512 (2015).
[33] Strictly speaking, these droplets are out of equilibrium because there is a flux of heat across them.
[34] J. Yoshioka, F. Ito, Y. Suzuki, H. Takahashi, H. Takizawa, and Y. Tabe, Director/barycentric rotation in cholesteric droplets under temperature gradient, Soft Matter **10**, 5869 (2014).
[35] G. Poy and P. Oswald, Do Lehmann cholesteric droplets subjected to a temperature gradient rotate as rigid bodies? Soft Matter **12**, 2604 (2015).
[36] U. Finkenzeller, T. Geelhaar, G. Weber, and L. Pohl, Liquid-crystalline reference compounds, Liq. Cryst. **5**, 313 (1989).
[37] P. Oswald, Lehmann rotation of cholesteric droplets subjected to a temperature gradient: Role of the concentration of chiral molecules, Eur. Phys. J. E **28**, 377 (2009).
[38] S. T. Wu and C. S. Wu, Rotational viscosity of nematic liquid crystals. A critical examination of existing models, Liq. Cryst. **8**, 171 (1990).
[39] P. Oswald and C. Scalliet, Measurements of the dielectric and viscoelastic constants in mixture of 4-4′-*n*-octyl-cyanobiphenyl and byphenyl, Phys. Rev. E **89**, 032504 (2014).
[40] P. Oswald, Easy axis memorization with active control of the azimuthal anchoring energy in nematic liquid crystals, Europhys. Lett. **107**, 26003 (2014).
[41] M. Marinelli, F. Mercuri, U. Zammit, and F. Scudieri, Thermal conductivity and thermal diffusivity of the cyanobiphenyl (nCB) homologous series, Phys. Rev. E **58**, 5860 (1998).
[42] P. Oswald, L. Jørgensen, and A. Żywociński, Lehmann rotatory power: A new concept in cholesteric liquid crystals, Liq. Cryst. **38**, 601 (2011).
[43] K. Denolf, G. Cordoyiannis, C. Glorieux, and J. Thoen, Effect of nonmesogenic impurities on the liquid crystalline phase transitions of octylcyanobiphenyl, Phys. Rev. E **76**, 051702 (2007).
[44] J. W. Kim, H. Kim, M. Lee, and J. J. Magda, Interfacial tension of a nematic liquid crystal/water interface with homeotropic surface alignment, Langmuir **20**, 8110 (2004).
[45] J. Ignés-Mullol and P. Oswald, Growth and melting of the nematic phase: Sample thickness dependence of the Mullins-Sekerka instability, Phys. Rev. E **61**, 3969 (2000).
[46] P. Oswald and G. Poy, Lehmann rotation of cholesteric droplets: Role of the sample thickness and of the concentration of chiral molecules, Phys. Rev. E **91**, 032502 (2015).
[47] M. A. Rahman and M. Z. Saghir, Thermodiffusion or Soret effect: Historical review, Int. J. Heat Mass Transf. **73**, 693 (2015).
[48] M. Škarabot, Ž. Lokar, and I. Muševič, Transport of particles by a thermally induced gradient of the order parameter in nematic liquid crystals, Phys. Rev. E **87**, 062501 (2013).
[49] A. Dequidt, G. Poy, and P. Oswald, Generalized drift velocity of a cholesteric texture in a temperature gradient, Soft Matter **12**, 7529 (2016).
[50] T. Yamamoto and M. Sano, Chirality-induced helical self-propulsion of cholesteric liquid crystal droplets, Soft Matter **13**, 3328 (2017).
[51] T. Yamamoto and M. Sano, Theoretical model of chirality-induced helical self-propulsion, Phys. Rev. E **97**, 012607 (2018).